Supplement of Hydrol. Earth Syst. Sci., 26, 1507–1525, 2022
https://doi.org/10.5194/hess-26-1507-2022-supplement

Hydrology and Earth System Sciences
Open Access
EGU

Supplement of

Theoretical and empirical evidence against the Budyko catchment trajectory conjecture

Nathan G. F. Reaver et al.

Correspondence to: Nathan G. F. Reaver (nreaver@ufl.edu)

S1 Introduction

The following items support the main text of the manuscript:

1) Figure S1 provides the locations of the UK and US reference catchments used in the empirical test of the catchment trajectory conjecture.
2) Table S1 lists studies that have developed relationships for the catchment-specific parameters, n or w, in terms of biophysical features, as well as their explicit equations.
3) Section S2 provides supplemental information for empirically testing for Budyko curve trajectories.
4) Section S3 provides supplemental information for the non-uniqueness of the parametric Budyko equations.
5) Section S4 provides supplemental information for interpreting n and w as proxy variables for the evaporative index.
6) Figure S2 illustrates n and w as proxy variables for the evaporative index.

The variable notation of the main text was updated from the original submission to comply with the journal's house standards, however, the variable notation of the original submission is maintained in this document. The relationships between the main text's notation and this document's notation are provided here:

- Potential evapotranspiration, E_0 (this document)
- Evapotranspiration, E (this document)
- Precipitation, P (this document)
- Discharge, Q (this document)
- Change in storage, ΔS (this document)
- Long-term mean potential evapotranspiration, PET (main text) and $\overline{E_0}$ (this document)
- Long-term mean evapotranspiration, ET (main text) and $\bar{E}$ (this document)
- Long-term mean precipitation, P (main text) and $\bar{P}$ (this document)
- Long-term mean discharge, Q (main text) and $\bar{Q}$ (this document)
- Long-term mean change in storage, ΔS (main text) and $\overline{\Delta S}$ (this document)

S2 Supplemental information for empirically testing for Budyko curve trajectories

Here we give more specific details of the methods used in the empirical test of the catchment trajectory conjecture, which consisted of following steps:

1) Computing the time series of E_0 for the US reference catchments
2) Calculating the expected Budyko curve catchment trajectories
3) Calculating the multiple realizations of actual catchment trajectories

4) Statistically comparing actual and expected catchment trajectories

S2.1 Computing the time series of E_0 for the US reference catchments

The 660 US references catchments used in the empirical test of the catchment trajectory conjecture were from the CAMELS dataset (Addor et al., 2017; Newman et al., 2015). Daily time series of T_{max} and T_{min} were available for each watershed, which allowed for the calculation of E_0 daily time series using the Hargreaves potential evaporation equation (Hargreaves and Allen, 2003; Lu et al., 2005);

$$E_0 = \begin{cases} [0.023]R_a\left[\frac{T_{max}+T_{min}}{2}+17.8\right]\sqrt{T_{max}+T_{min}}, & \frac{T_{max}+T_{min}}{2} > -17.8 \\ 0, & \frac{T_{max}+T_{min}}{2} \leq -17.8 \end{cases}, \quad \text{(S1)}$$

where E_0 is the potential evapotranspiration in mm/day, T_{max} is the maximum daily temperature in degrees Celsius, T_{min} is the minimum daily temperature in degrees Celsius, and R_a is the extraterrestrial radiation in MJ/m^2/day. Daily R_a estimates were calculated using the catchments' latitude and the equations for "extraterrestrial radiation for daily periods" (Allen et al. (1998).

S2.2 Calculating the expected Budyko curve catchment trajectories

The expected Budyko curve trajectories were calculated by fitting Eq. (5) of the main text to the long-term values of $\frac{\overline{E_0}}{\bar{P}}$ and $\frac{\bar{E}}{\bar{P}}$ for each catchment. Long-term values of $\frac{\overline{E_0}}{\bar{P}}$ and $\frac{\bar{E}}{\bar{P}}$ were calculated from $\overline{E_0}$, $\bar{P}$, and $\bar{E}$, which were estimated using the entire period of record of daily Q, P, and E_0 values. Specifically,

$$\bar{P} = \frac{1}{N}\sum_{i=1}^{N} P_i \,, \quad \text{(S2)}$$

$$\overline{E_0} = \frac{1}{N}\sum_{i=1}^{N} E_{0_i} \,, \quad \text{(S3)}$$

and

$$\bar{E} = \bar{P} - \bar{Q} = \bar{P} - \frac{1}{N}\sum_{i=1}^{N} Q_i \,, \quad \text{(S4)}$$

where P_i, E_{0_i}, and Q_i are the daily values of P, E_0, and Q, respectively, and N is the total number of days in the catchment's record. The expected Budyko curve trajectories are defined by Eq. (5) with a fitted value of the catchment-specific parameter n obtained by numerically solving

$$\left[\frac{\frac{\overline{E_0}}{\bar{P}}}{\left[1+\left(\frac{\overline{E_0}}{\bar{P}}\right)^n\right]^{\frac{1}{n}}} - \frac{\bar{E}}{\bar{P}}\right]^2 = 0 \,. \quad \text{(S5)}$$

The fitted n values were used to generate the expected location of the catchments in Budyko space for any value of $\frac{\overline{E_0}}{\bar{P}}$.

S2.3 Calculating the multiple realizations of actual catchment trajectories

The actual trajectories that the reference catchments took through Budyko space were determined by calculating the temporally sequential values of $\frac{\overline{E_0}}{\bar{P}}$ and $\frac{\bar{E}}{\bar{P}}$, using averaging windows varying from 1 year to the maximum number of whole years in the catchment's record (ranging between 1 to 11 years and 1 to 56 years). For example, if a reference catchment had a period of record of length 25.5 years, it would have 25 realizations of the actual trajectory it took through Budyko space, one for each averaging window between 1 and 25 years. This resulted in a sum total of 24,501 realizations from the 728 reference catchments.

The actual Budyko space trajectories, consisting of temporally sequential values of $\frac{\overline{E_0}}{\bar{P}}$ and $\frac{\bar{E}}{\bar{P}}$, were calculated from temporally sequential values $\overline{E_0}$, $\bar{P}$, and $\bar{E}$, which were estimated using the records of daily Q, P, and E_0 values. Specifically,

$$Ж_M = \left\{ \left(\frac{\frac{1}{M}\sum_{i=1}^{M} E_{0i}}{\frac{1}{M}\sum_{i=1}^{M} P_i}, \frac{\frac{1}{M}\sum_{i=1}^{M} P_i - Q_i}{\frac{1}{M}\sum_{i=1}^{M} P_i} \right), \left(\frac{\frac{1}{M}\sum_{i=2}^{M+1} E_{0i}}{\frac{1}{M}\sum_{i=2}^{M+1} P_i}, \frac{\frac{1}{M}\sum_{i=2}^{M+1} P_i - Q_i}{\frac{1}{M}\sum_{i=2}^{M+1} P_i} \right), \cdots, \left(\frac{\frac{1}{M}\sum_{i=N-M+1}^{N} E_{0i}}{\frac{1}{M}\sum_{i=N-M+1}^{N} P_i}, \frac{\frac{1}{M}\sum_{i=N-M+1}^{N} P_i - Q_i}{\frac{1}{M}\sum_{i=N-M+1}^{N} P_i} \right) \right\}, \quad \text{(S6)}$$

where $Ж_M$ is actual Budyko space trajectory realization for averaging window size M, comprised of the set, { }, of temporally sequential values of $\frac{\overline{E_0}}{\bar{P}}$ and $\frac{\bar{E}}{\bar{P}}$, (,). P_i, E_{0_i}, Q_i, and N are the same as defined in Sect. S2.2.

S2.4 Statistically comparing actual and expected catchment trajectories

The catchment trajectory conjecture was tested for each realization of the reference catchments' actual trajectories (i.e., $Ж_M$) by statistically comparing them to the corresponding expected Budyko curve trajectories using the non-parametric sign test (Holander and Wolfe, 1973). The sign test is sensitive to the presence of consistent differences between paired observations and requires few assumptions, which makes it widely applicable. Specifically, for the test between the expected and actual Budyko space catchment trajectories, the assumptions are: 1) $Z_k = Y_k - X_k$ and $Z_k = \theta + \epsilon_k$; where $Y_k = \frac{\frac{1}{M}\sum_{i=k}^{M+k-1} P_i - Q_i}{\frac{1}{M}\sum_{i=k}^{M+k-1} P_i}$ and $X_k = \frac{\frac{\frac{1}{M}\sum_{i=k}^{M+k-1} E_{0i}}{\frac{1}{M}\sum_{i=k}^{M+k-1} P_i}}{\left[1+\left(\frac{\frac{1}{M}\sum_{i=k}^{M+k-1} E_{0i}}{\frac{1}{M}\sum_{i=k}^{M+k-1} P_i}\right)^n\right]^{\frac{1}{n}}}$ are the paired actual and expected evaporative index observations, respectively; P_i, E_{0_i}, Q_i, N, and M are the same as defined in Sect. S2.2 and Sect. S2.3; n is the fitted value of the catchment-specific parameter obtained from Eq. (S5) in Sect. S2.2; $k = 1,2,3,\cdots,N-M+1$; θ is the size of the unknown consistent differences between actual and expected trajectories; and ϵ_k is the unobserved random effects associated with each pair of actual and expected evaporative index observations. 2) $\{\epsilon_k\}$ are mutually independent. 3) Each ϵ_k comes from a continuous population with a median zero, though not necessarily the same distribution.

The null hypothesis for the sign test is,

$$H_0: \theta = 0\ , \tag{S7}$$

which is that there is no consistent difference between the actual and expected Budyko space trajectories. To test H_0, we first compute the statistic,

$$B = \sum_{k=1}^{N-M+1} \chi_k\ , \tag{S8}$$

where $\chi_k = \begin{cases} 1, & Z_k > 0 \\ 0, & Z_k < 0 \end{cases}$. Under the null hypothesis, B is distributed binomially, specifically, $B \sim \frac{(N-M+1)!}{B!(N-M+1-B)!}\left[\frac{1}{2}\right]^{N-M+1}$, which has the cumulative distribution function,

$$p = I_{\frac{1}{2}}(N - M + 1 - B, 1 + B)\ , \tag{S9}$$

where $I_x(\ ,\ )$ is the regularized incomplete beta function. We reject the null hypothesis at the 0.95 confidence level, in favor of the alternative hypothesis, $H_1: \theta \neq 0$ (i.e., there is a consistent difference between the actual and expected Budyko space trajectories), if, $I_{\frac{1}{2}}(N - M + 1 - B, 1 + B) < 0.025$ or $I_{\frac{1}{2}}(N - M + 1 - B, 1 + B) > 0.975$.

S2.5 Controlling for potential catchment storage dynamics

The temporal averaging window for which $\overline{\Delta S} \approx 0$ for the reference catchments in this study is unknown and may vary between catchments. However, it should be expected that above some threshold averaging window size, $\overline{\Delta S} \approx 0$ for many of the catchments most of the time (e.g., greater than a 10 year-average window), otherwise the reference catchments would rarely be in steady state. This threshold behaviour for $\overline{\Delta S} \approx 0$ has been shown to be near universal for catchments across Earth (Han et al., 2020), however, even if this was not the case for our reference catchments, and they are rarely in steady state, it should be expected that for some averaging windows for some catchments, steady state conditions are present (i.e., $\overline{\Delta S} \approx 0$). With or without this threshold behavior, testing all of the averaging windows for all catchments allows for a robust test of the catchment trajectory conjecture. In the case of threshold behavior, once the averaging window has reached sufficient size for a particular catchment (e.g., > 10 years), if the catchment trajectory conjecture is correct, the actual and expected Budyko space trajectories would be consistently statistically indistinguishable. This means that the frequency at which actual and expected Budyko space trajectories are found to be statistically indistinguishable would be higher than what would be expected due to random chance (i.e., more than 5% of all the possible actual and expected Budyko space trajectories would be statistically indistinguishable at a significance level of 0.05). An elevated frequency of statistical similarity would also occur if catchments were only rarely in steady state. The reason for this elevation is that the number of statistically similar trajectories from averaging windows where $\overline{\Delta S} \approx 0$ would be in addition to the number of statistically similar trajectories expected from random chance.

S2.6 The insensitivity of the empirical test methodology to the choice of E_0

The methodology for the empirical test of the catchment trajectory conjecture is insensitive to the choice of E_0 method. There are three primary reasons for this: (1) the various possible E_0 methods that could be used in this analysis are highly correlated, so the choice of method will not alter the basic shape of the actual Budyko space trajectories; (2) for all averaging periods, catchments' trajectories are overwhelmingly driven by changes in $\bar{P}$ rather than changes in $\overline{E_0}$, so the choice of E_0 method will not alter the basic shape of the actual Budyko space trajectories; and (3) the non-parametric sign test used to determine consistent differences between actual and expected trajectories will provide near-identical results for each possible E_0 method if the basic shape of the actual Budyko space trajectories are generally preserved. We summarize each of these below.

(1) While various E_0 methods may differ in magnitude, most methods (e.g., pan-, temperature-, radiation-, and mass transfer-based) are highly correlated. This high degree of correlation means that any one particular method can be well approximated as a linear function of any other (i.e., $E_0^1 = \alpha E_0^2 + \beta$). Different choices of E_0 methods can thus only do two things to a catchment's actual Budyko space trajectory, translate the entire trajectory along the ϕ axis and/or symmetrically expand or contract the trajectory around its average value in the ϕ dimension. Neither of these operations changes the basic shape of the trajectory for different E_0 methods, making the conclusions obtained from our catchment trajectory conjecture test largely insensitive to the choice of E_0 method.

(2) A catchment's actual trajectory through Budyko space is overwhelmingly driven by changes in $\bar{P}$ rather than changes in $\overline{E_0}$. This is because annual average E_0 is very consistent from year to year regardless of E_0 method used. In our analysis, we used all possible averaging windows, ranging from 1 to 45 years, to compute time varying values of $\overline{E_0}$ and $\bar{P}$, which were used to produce all possible actual catchment trajectory realizations. For almost possible all realizations, the variation in $\bar{P}$ will be far greater than the variation in $\overline{E_0}$. This implies that changes in a catchment's ϕ (i.e., the ϕ axis the component of its Budyko space trajectory) is primarily driven by changes in $\bar{P}$. Since the temporal dynamics of $\overline{E_0}$ are much less important than those of $\bar{P}$ in determining actual trajectories, the choice of E_0 method has little impact on shape of actual trajectories.

(3) The non-parametric sign test used in the empirical analysis (see Sect. S2.4) tests for consistent over- or under-estimation between paired observations (i.e., the actual and expected trajectories). If the catchment trajectory conjecture is correct, the catchment's actual trajectory would not be consistently greater than or less than the expected trajectory (i.e., they would be statistically indistinguishable). If a catchment's actual and expected trajectories are statistically similar when one particular E_0 method is used, then based on the previous two reasons above, this statistical similarity will almost always be maintained for any E_0 method.

The basic shape of an actual trajectory determines whether or not it is consistently above or below the expected trajectory. Since $\overline{E_0}$ does not vary much over time and because the various E_0 methods are highly correlated, changing the E_0 method

will not alter the basic shape of the actual trajectory. The actual trajectory could expand or contract in the ϕ dimension, however, because these operations are symmetric, they will not alter the frequency at which the trajectory is above or below the expected trajectory. Changing the E_0 method could cause the actual and expected trajectories to be translated along the ϕ axis. While this operation would not change the shape of the actual trajectory, it would change the expected trajectory since the long-term mean values of ϕ and the evaporative index fall on a new parametric Budyko curve. The new expected trajectory will be slightly rotated with respect to actual trajectory as compared to the trajectories with original E_0 method. This slight rotation will cause the actual trajectory to be above and below the expected trajectory slightly more frequently, but the relative frequency of over- and under-estimation will be unchanged in most cases.

Thus for any particular choice of E_0 method, the relative frequency of over- and under-estimation remains almost constant for all potential alterations of the actual or expected trajectories. The outcome of the non-parametric sign test is dependent on this relative frequency, meaning its results are robust against the choice of different E_0 methods.

S3 Supplemental information for the non-uniqueness of the parametric Budyko equations

S3.1 Generating parametric Budyko equations

Here we provide a method to generate single parameter Budyko equations and use it to produce Eq. (14) and (15) in the main text. It is important to note that the equations generated through this method are arbitrary and under-determined in the same way as Eq. (5) and (6), therefore, we do not advocate their use as a predictive tool within catchment hydrology. Their purpose is only to illustrate the non-uniqueness of single parameter Budyko equations (such as Eq. (5) and (6)).

To be a valid parametric Budyko equation analogous to Eq. (5) and (6) in the main text, an equation should: 1) approach 0 and 1 in the humid (i.e. $\phi \to 0$) and arid (i.e. $\phi \to \infty$) limits, respectively; 2) have its first derivative approach 1 and 0 in the humid (i.e. $\phi \to 0$) and arid (i.e. $\phi \to \infty$) limits, respectively; 3) asymptotically approach the energy and water limits as the catchment-specific parameter approaches infinity; and 4) asymptotically approach zero as the catchment-specific parameter approaches its lower bound; Any other single-parameter equation in addition to Eq. (5) and (6) that has these properties could be an equally valid parametric "Budyko equation".

To generate valid parametric Budyko equations, first, we assume the aridity index, ϕ, is the first moment of an underlying distribution which describes the frequency of observing a given instantaneous aridity, ϕ, for a catchment (i.e., $\phi = \bar{\phi}$). This instantaneous aridity variable is always positive or zero (i.e., $\phi \geq 0$). From ϕ and conservation of energy and mass we can define an instantaneous evaporative variable as,

$$\varepsilon = \begin{cases} \phi, & \phi < 1 \\ 1, & \phi \geq 1 \end{cases}. \tag{S10}$$

The evaporative index is the first moment of the instantaneous evaporative distribution (i.e., $\frac{\bar{E}}{\bar{P}} = \bar{\varepsilon}$), which can be written as,

$$\frac{\bar{E}}{\bar{P}} = \bar{\varepsilon} = \rho_{\phi\geq1}\overline{\phi}_{\phi\geq1} + \rho_{\phi<1}\overline{\phi}_{\phi<1}, \tag{S11}$$

where $\rho_{\phi\geq1}$ is the truncated zeroth moment of the instantaneous aridity distribution for $\phi \geq 1$, $\overline{\phi}_{\phi\geq1}$ is the truncated first moment of the instantaneous aridity distribution for $\phi \geq 1$, $\rho_{\phi<1}$ is the truncated zeroth moment of the instantaneous aridity distribution for $\phi < 1$, and $\overline{\phi}_{\phi<1}$ is the truncated first moment of the instantaneous aridity distribution for $\phi < 1$. Since, $\overline{\phi}_{\phi\geq1} = 1$ and $\rho_{\phi\geq1} = 1 - \rho_{\phi<1}$, Eq. (S11) can be further simplified to,

$$\frac{\bar{E}}{\bar{P}} = \bar{\varepsilon} = 1 - \rho_{\phi<1} + \rho_{\phi<1}\overline{\phi}_{\phi<1}. \tag{S12}$$

Equation (S12) can be used to generate distinct valid parametric Budyko equations by specifying a particular non-negative two-parameter distribution for ϕ and analytically solving $\rho_{\phi<1}$ and $\overline{\phi}_{\phi<1}$ in terms of ϕ and a second, appropriately chosen catchment-specific parameter, q.

S3.2 Choice of ϕ distribution and q for Eq. (14)

To produce Eq. (14) in the main text, we use Eq. (S12) with the choice of a two-parameter distribution for ϕ, the gamma distribution,

$$\phi \sim \frac{\beta^{\alpha}}{\Gamma(\alpha)}\phi^{\alpha-1}e^{-\beta\phi}, \tag{S13}$$

where the shape parameter, $\alpha > 0$, the rate parameter, $\beta > 0$, and $\Gamma(\ )$ is the gamma function. The parameters $\rho_{\phi<1}$ and $\overline{\phi}_{\phi<1}$ of Eq. (S12) are defined as follows for the gamma distribution,

$$\rho_{\phi<1} = \frac{\gamma(\alpha,\beta)}{\Gamma(\alpha)}, \tag{S14}$$

and

$$\overline{\phi}_{\phi<1} = \frac{\Gamma(\alpha)}{\gamma(\alpha,\beta)}\frac{\alpha}{\beta}\frac{\gamma(\alpha+1,\beta)}{\Gamma(\alpha+1)}, \tag{S15}$$

where $\gamma(\ ,\ )$ is the lower incomplete gamma function.

Next, we choose an appropriate attribute of the distribution of ϕ as the catchment-specific parameter, q, specifically,

$$q = \alpha. \tag{S16}$$

The mean of the gamma distribution can be expressed in terms of α and β, as $\phi = \frac{\alpha}{\beta}$. Solving these equations for α and β gives the gamma distribution parameters in terms of ϕ and q,

$$\alpha = q, \tag{S17}$$

and

$$\beta = \frac{\alpha}{\phi} = \frac{q}{\phi}, \tag{S18}$$

Substituting Eq. (S14), (S15), (S17), and (S18) into Eq. (S12) and letting $q = q_n$ yields,

$$\frac{\bar{E}}{\bar{P}} = 1 - \left[\frac{\gamma\left(q_n, \frac{q_n}{\phi}\right)}{\Gamma(q_n)}\right] + \left[\frac{\gamma\left(q_n+1, \frac{q_n}{\phi}\right)}{\Gamma(q_n+1)}\phi\right], \tag{S19}$$

which is Eq. (14) of the main text.

Now, we test the Eq. (14) to determine if it has the required properties to be a valid parametric Budyko equation analogous to Eq. (5) and (6). First, Eq. (14) should approach 0 and 1 in the humid (i.e. $\phi \to 0$) and arid (i.e. $\phi \to \infty$) limits, respectively. We can test these conditions by taking the appropriate limits of Eq. (S19),

$$\lim_{\phi \to 0}\left[1 - \left[\frac{\gamma\left(q_n, \frac{q_n}{\phi}\right)}{\Gamma(q_n)}\right] + \left[\frac{\gamma\left(q_n+1, \frac{q_n}{\phi}\right)}{\Gamma(q_n+1)}\phi\right]\right] = 1 - 1 + (1)(0) = 0, \tag{S20}$$

and

$$\lim_{\phi \to \infty}\left[1 - \left[\frac{\gamma\left(q_n, \frac{q_n}{\phi}\right)}{\Gamma(q_n)}\right] + \left[\frac{\gamma\left(q_n+1, \frac{q_n}{\phi}\right)}{\Gamma(q_n+1)}\phi\right]\right] = \lim_{\phi \to \infty}\left[1 - \left[\frac{\gamma\left(q_n, \frac{q_n}{\phi}\right)}{\Gamma(q_n)}\right] + \left[\frac{q_n\left[\frac{q_n}{\phi}\right]^{q_n} e^{-\frac{q_n}{\phi}}}{\Gamma(q_n+1)}\right]\right] = 1 - 0 + 0 = 1, \tag{S21}$$

which are the required values. Second, the first derivative of Eq. (14) should approach 1 and 0 in the humid (i.e. $\phi \to 0$) and arid (i.e. $\phi \to \infty$) limits, respectively. We can test these conditions by taking the appropriate limits of the derivative of Eq. (S19),

$$\frac{d\frac{\bar{E}}{\bar{P}}}{d\phi} = \frac{\gamma\left(q_n+1, \frac{q_n}{\phi}\right)}{\Gamma(q_n+1)}, \tag{S22}$$

which gives,

$$\lim_{\phi \to 0}\left[\frac{\gamma\left(q_n+1, \frac{q_n}{\phi}\right)}{\Gamma(q_n+1)}\right] = 1, \tag{S23}$$

and

$$\lim_{\phi \to \infty}\left[\frac{\gamma\left(q_n+1, \frac{q_n}{\phi}\right)}{\Gamma(q_n+1)}\right] = 0, \tag{S24}$$

which are the required values. Third, Eq. (14) should asymptotically approach the energy and water limits as the catchment-specific parameter approaches infinity. We test this condition by taking the limit of Eq. (S19) as $q_n \to \infty$, which gives,

$$\lim_{q_n\to\infty}\begin{cases}1-\left[\frac{\gamma\left(q_n,\frac{q_n}{\phi}\right)}{\Gamma(q_n)}\right]+\left[\frac{\gamma\left(q_n+1,\frac{q_n}{\phi}\right)}{\Gamma(q_n+1)}\phi\right], & \phi<1\\ 1-\left[\frac{\gamma\left(q_n,\frac{q_n}{\phi}\right)}{\Gamma(q_n)}\right]+\left[\frac{\gamma\left(q_n+1,\frac{q_n}{\phi}\right)}{\Gamma(q_n+1)}\phi\right], & \phi\geq 1\end{cases}=\begin{cases}1-1+(1)(\phi), & \phi<1\\ 1-0+(0)(\phi), & \phi\geq 1\end{cases}=\begin{cases}\phi, & \phi<1\\ 1, & \phi\geq 1\end{cases}, \tag{S25}$$

the water and energy limits. Finally, Eq. (14) should asymptotically approach zero as the catchment-specific parameter approaches its lower bound. By taking the limit of Eq. (S19) as $q_n \to 0$, we can test to see that it asymptotically approaches zero,

$$\lim_{q_n\to 0}\begin{cases}1-\left[\frac{\gamma\left(q_n,\frac{q_n}{\phi}\right)}{\Gamma(q_n)}\right]+\left[\frac{\gamma\left(q_n+1,\frac{q_n}{\phi}\right)}{\Gamma(q_n+1)}\phi\right], & \phi<1\\ 1-\left[\frac{\gamma\left(q_n,\frac{q_n}{\phi}\right)}{\Gamma(q_n)}\right]+\left[\frac{\gamma\left(q_n+1,\frac{q_n}{\phi}\right)}{\Gamma(q_n+1)}\phi\right], & \phi\geq 1\end{cases}=\begin{cases}1-1+(0)(\phi), & \phi<1\\ 1-1+(0)(\phi), & \phi\geq 1\end{cases}=\begin{cases}0, & \phi<1\\ 0, & \phi\geq 1\end{cases}. \tag{S26}$$

Thus, Eq. (14) satisfies all requirements for a valid parametric Budyko equation.

S3.3 Choice of ϕ distribution and q for Eq. (15)

To produce Eq. (15) in the main text, we use Eq. (S12) with the choice of a two-parameter distribution for ϕ, the Nakagami distribution,

$$\phi\sim\frac{2m^m}{\Gamma(m)\Omega^m}\phi^{2m-1}e^{-\frac{m}{\Omega}\phi^2}, \tag{S27}$$

where the shape parameter, $m>0$, and the spread parameter, $\Omega>0$. The parameters $\rho_{\phi<1}$ and $\overline{\phi}_{\phi<1}$ of Eq. (S12) are defined as follows for the Nakagami distribution,

$$\rho_{\phi<1}=\frac{\gamma\left(m,\frac{m}{\Omega}\right)}{\Gamma(m)}, \tag{S28}$$

and

$$\overline{\phi}_{\phi<1}=\frac{\Gamma(m)}{\gamma\left(m,\frac{m}{\Omega}\right)}\frac{\Gamma\left(m+\frac{1}{2}\right)}{\Gamma(m)}\sqrt{\frac{\Omega}{m}}\frac{\gamma\left(m+\frac{1}{2},\frac{m}{\Omega}\right)}{\Gamma\left(m+\frac{1}{2}\right)}. \tag{S29}$$

Next, we choose an appropriate attribute of the distribution of ϕ as the catchment-specific parameter, q, specifically,

$$q=m+1. \tag{S30}$$

The mean of Nakagami distribution can be expressed in terms of m and Ω as,

$$\phi=\frac{\Gamma\left(m+\frac{1}{2}\right)}{\Gamma(m)}\sqrt{\frac{\Omega}{m}}. \tag{S31}$$

Solving these equations for m and Ω gives the Nakagami distribution parameters in terms of ϕ and q,

$$m = q - 1\,, \tag{S32}$$

and

$$\Omega = \frac{\phi^2[q-1]\Gamma(q-1)}{\Gamma\left(q-\frac{1}{2}\right)}\,, \tag{S33}$$

Substituting Eq. (S28), (S29), (S32), and (S33) into Eq. (S12) and letting $q = q_w$ yields,

$$\frac{\bar{E}}{\bar{P}} = 1 - \left[\frac{\gamma\left(q_w-1,\frac{\Gamma\left(q_w-\frac{1}{2}\right)}{\phi^2\Gamma(q_w-1)}\right)}{\Gamma(q_w-1)}\right] + \left[\frac{\gamma\left(q_w-\frac{1}{2},\frac{\Gamma\left(q_w-\frac{1}{2}\right)}{\phi^2\Gamma(q_w-1)}\right)}{\Gamma\left(q_w-\frac{1}{2}\right)}\phi\right], \tag{S34}$$

which is Eq. (15) of the main text.

Now, we test the Eq. (15) to determine if it has the required properties to be a valid parametric Budyko equation analogous to Eq. (5) and (6). First, Eq. (15) should approach 0 and 1 in the humid (i.e. $\phi \to 0$) and arid (i.e. $\phi \to \infty$) limits, respectively. We can test these conditions by taking the appropriate limits of Eq. (S34),

$$\lim_{\phi\to 0}\left[1 - \left[\frac{\gamma\left(q_w-1,\frac{\Gamma\left(q_w-\frac{1}{2}\right)}{\phi^2\Gamma(q_w-1)}\right)}{\Gamma(q_w-1)}\right] + \left[\frac{\gamma\left(q_w-\frac{1}{2},\frac{\Gamma\left(q_w-\frac{1}{2}\right)}{\phi^2\Gamma(q_w-1)}\right)}{\Gamma\left(q_w-\frac{1}{2}\right)}\phi\right]\right] = 1 - 1 + (1)(0) = 0\,, \tag{S35}$$

and

$$\lim_{\phi\to\infty}\left[1 - \left[\frac{\gamma\left(q_w-1,\frac{\Gamma\left(q_w-\frac{1}{2}\right)}{\phi^2\Gamma(q_w-1)}\right)}{\Gamma(q_w-1)}\right] + \left[\frac{\gamma\left(q_w-\frac{1}{2},\frac{\Gamma\left(q_w-\frac{1}{2}\right)}{\phi^2\Gamma(q_w-1)}\right)}{\Gamma\left(q_w-\frac{1}{2}\right)}\phi\right]\right] = 1 - 0 + \lim_{\phi\to\infty}\left[\frac{2\left[\frac{\Gamma\left(q_w-\frac{1}{2}\right)}{\Gamma(q_w-1)}\right]^{\left[q_w-\frac{1}{2}\right]} e^{-\frac{\Gamma\left(q_w-\frac{1}{2}\right)}{\phi^2\Gamma(q_w-1)}}}{[\phi]^{[2q_w-1]}\Gamma\left(q_w-\frac{1}{2}\right)}\right] = 1 + 0 = 1, \tag{S36}$$

which are the required values. Second, the first derivative of Eq. (15) should approach 1 and 0 in the humid (i.e. $\phi \to 0$) and arid (i.e. $\phi \to \infty$) limits, respectively. We can test these conditions by taking the appropriate limits of the derivative of Eq. (S34),

$$\frac{d\frac{\bar{E}}{\bar{P}}}{d\phi} = \frac{\gamma\left(q_w-\frac{1}{2},\frac{\Gamma\left(q_w-\frac{1}{2}\right)}{\phi^2\Gamma(q_w-1)}\right)}{\Gamma\left(q_w-\frac{1}{2}\right)}, \tag{S37}$$

which gives,

$$\lim_{\phi\to 0}\left[\frac{\gamma\left(q_w-\frac{1}{2},\frac{\Gamma\left(q_w-\frac{1}{2}\right)}{\phi^2\Gamma(q_w-1)}\right)}{\Gamma\left(q_w-\frac{1}{2}\right)}\right] = 1\,, \tag{S38}$$

and

$$\lim_{\phi\to\infty}\left[\frac{\gamma\left(q_w-\frac{1}{2},\frac{\Gamma\left(q_w-\frac{1}{2}\right)}{\phi^2\Gamma(q_w-1)}\right)}{\Gamma\left(q_w-\frac{1}{2}\right)}\right]=0\,, \tag{S39}$$

which are the required values. Third, Eq. (15) should asymptotically approach the energy and water limits as the catchment-specific parameter approaches infinity. We test this condition by taking the limit of Eq. (S34) as $q_w\to\infty$, which gives,

$$\lim_{q_w\to\infty}\begin{cases}1-\left[\frac{\gamma\left(q_w-1,\frac{\Gamma\left(q_w-\frac{1}{2}\right)}{\phi^2\Gamma(q_w-1)}\right)}{\Gamma(q_w-1)}\right]+\left[\frac{\gamma\left(q_w-\frac{1}{2},\frac{\Gamma\left(q_w-\frac{1}{2}\right)}{\phi^2\Gamma(q_w-1)}\right)}{\Gamma\left(q_w-\frac{1}{2}\right)}\phi\right],\ \phi<1\\ 1-\left[\frac{\gamma\left(q_w-1,\frac{\Gamma\left(q_w-\frac{1}{2}\right)}{\phi^2\Gamma(q_w-1)}\right)}{\Gamma(q_w-1)}\right]+\left[\frac{\gamma\left(q_w-\frac{1}{2},\frac{\Gamma\left(q_w-\frac{1}{2}\right)}{\phi^2\Gamma(q_w-1)}\right)}{\Gamma\left(q_w-\frac{1}{2}\right)}\phi\right],\ \phi\geq1\end{cases}=\begin{cases}1-1+(1)(\phi),\ \phi<1\\ 1-0+(0)(\phi),\ \phi\geq1\end{cases}=\begin{cases}\phi,\ \phi<1\\ 1,\ \phi\geq1\end{cases}, \tag{S40}$$

the water and energy limits. Finally, Eq. (15) should asymptotically approach zero as the catchment-specific parameter approaches its lower bound. By taking the limit of Eq. (S34) as $q_w\to1$, we can test to see that it asymptotically approaches zero,

$$\lim_{q_w\to1}\begin{cases}1-\left[\frac{\gamma\left(q_w-1,\frac{\Gamma\left(q_w-\frac{1}{2}\right)}{\phi^2\Gamma(q_w-1)}\right)}{\Gamma(q_w-1)}\right]+\left[\frac{\gamma\left(q_w-\frac{1}{2},\frac{\Gamma\left(q_w-\frac{1}{2}\right)}{\phi^2\Gamma(q_w-1)}\right)}{\Gamma\left(q_w-\frac{1}{2}\right)}\phi\right],\ \phi<1\\ 1-\left[\frac{\gamma\left(q_w-1,\frac{\Gamma\left(q_w-\frac{1}{2}\right)}{\phi^2\Gamma(q_w-1)}\right)}{\Gamma(q_w-1)}\right]+\left[\frac{\gamma\left(q_w-\frac{1}{2},\frac{\Gamma\left(q_w-\frac{1}{2}\right)}{\phi^2\Gamma(q_w-1)}\right)}{\Gamma\left(q_w-\frac{1}{2}\right)}\phi\right],\ \phi\geq1\end{cases}=\begin{cases}1-1+(0)(\phi),\ \phi<1\\ 1-1+(0)(\phi),\ \phi\geq1\end{cases}=\begin{cases}0,\ \phi<1\\ 0,\ \phi\geq1\end{cases}. \tag{S41}$$

Thus, Eq. (15) satisfies all requirements for a valid parametric Budyko equation.

S4 Supplemental information for interpreting n and w as proxy variables for the evaporative index

S4.1 Level curve expressions of the dependence between n, w, and the evaporative index

Here we formally express the proxy nature of n or w and $\frac{\bar{E}}{\bar{P}}$ in terms of level curves. Level curves can be expressed in the form,

$$L_c(f)=\{(x_1,x_2)|f(x_1,x_2)=c\}\,, \tag{S42}$$

which describes the set, { }, of values of the real variables x_1 and x_2 given a function, f, that is equal to a constant, c. Applying this general form to the parametric Budyko equations for a particular ϕ yields,

$$L_\phi(f_3) = \left\{\left(n, \frac{\bar{E}}{\bar{P}}\right) \middle| f_3\left(n, \frac{\bar{E}}{\bar{P}}\right) = \phi\right\}, \tag{S43}$$

and

$$L_\phi(f_4) = \left\{\left(w, \frac{\bar{E}}{\bar{P}}\right) \middle| f_4\left(w, \frac{\bar{E}}{\bar{P}}\right) = \phi\right\}, \tag{S44}$$

where

$$f_3\left(n, \frac{\bar{E}}{\bar{P}}\right) = \left[\frac{\bar{E}}{\bar{P}}\right][1 + (\phi)^n]^{\frac{1}{n}}, \tag{S45}$$

and

$$f_4\left(w, \frac{\bar{E}}{\bar{P}}\right) = \frac{\bar{E}}{\bar{P}} - 1 + (1 + (\phi)^w)^{\frac{1}{w}}. \tag{S46}$$

Eq. (S43) and (S44) directly define the dependent relationship between n and w and $\frac{\bar{E}}{\bar{P}}$, respectively. These level curves are plotted in Fig. S2.

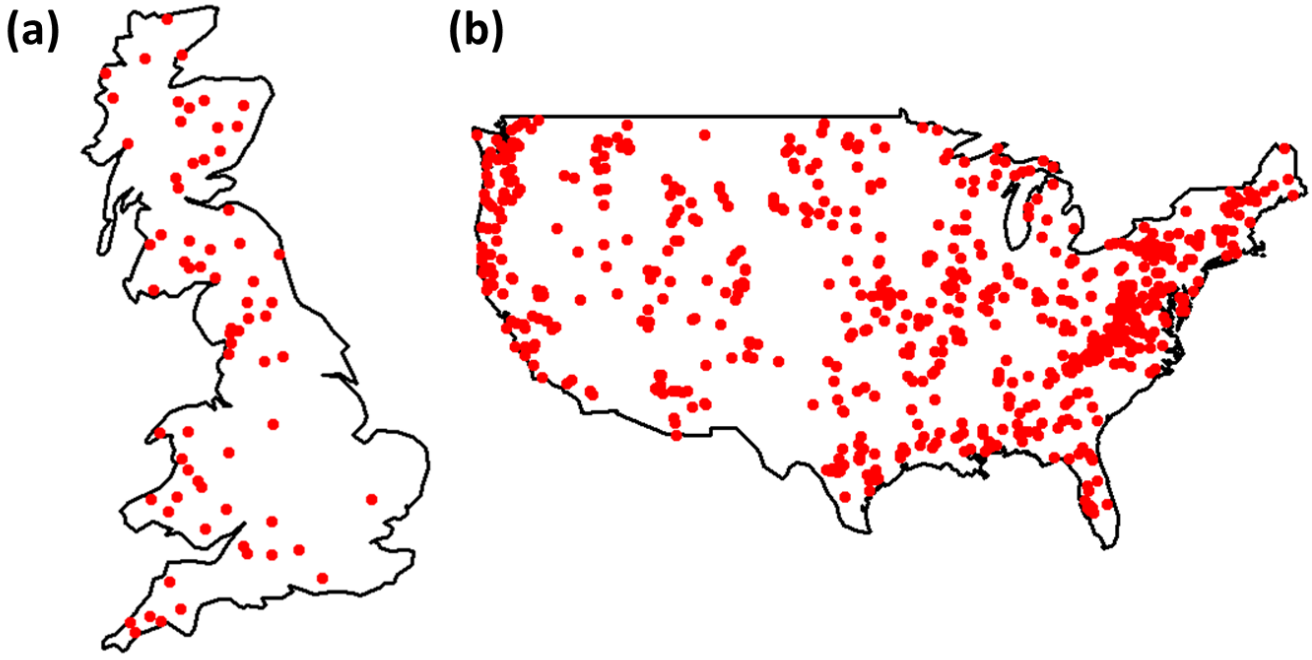

Figure S1: Reference catchments (red dots) used in the empirical test of the catchment trajectory conjecture. The reference catchments are known to have stable unchanging land use over the length of their Q, P, and E_0 records. (a) Great Britain with the

locations of 68 UK reference catchments from the CAMELS-GB and UKBN2 datasets. (b) The US with the locations of the 660 reference catchments from the CAMELS dataset.

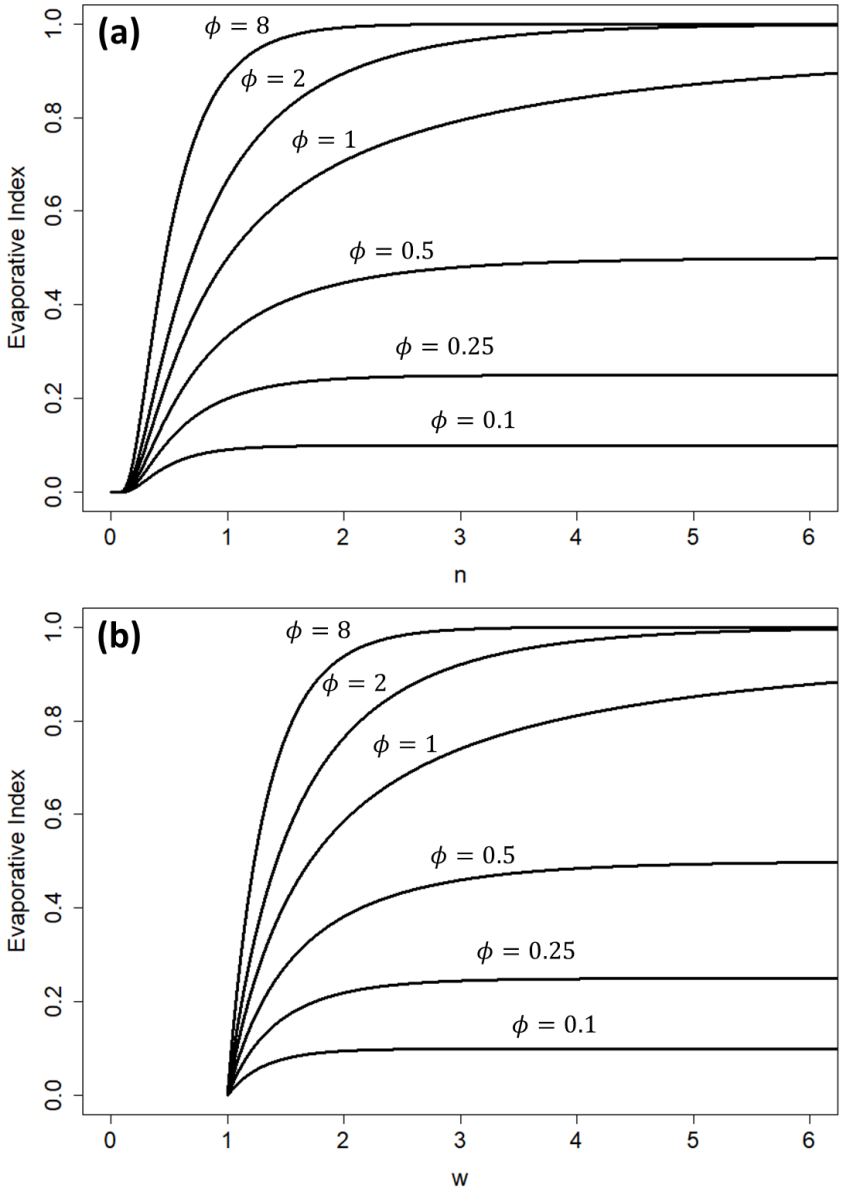

Figure S2: Illustration of the catchment-specific parameters as proxy variables for the evaporative index. For a given aridity index (ϕ) the evaporative index completely determines the catchment-specific parameter (w or n) through a one-to-one relationship. (a) Level curves described by Eq. (S43). (b) Level curves described by Eq. (S44).

Table S1: Existing relationships for the catchment-specific parameter in terms of biophysical features. Variables in each of the expressions are defined within the table. Complicated statistical expressions not amenable to tabulation are listed as a general function, $F(\ )$, of the statistically significant variables, with details available in the cited work.

Functional Forms	Parameters	Methodology	Reference
$w = 1 + 8.852\left(\frac{K_s}{\overline{i_r}}\right)^{-0.368}\left(\frac{S_{max}}{\overline{E_0}}\right)^{0.436} e^{-4.464\tan\beta}$ and $w = 2.947 - 0.55\left(\frac{K_s}{\overline{i_r}}\right) + 0.882\left(\frac{S_{max}}{\overline{E_0}}\right) - 2.096\tan\beta$	K_s, saturated hydraulic conductivity $\overline{i_r}$, mean precipitation intensity in 24 hours S_{max}, plant extractable water capacity $\overline{E_0}$, mean annual potential evapotranspiration $\tan\beta$, average slope	Optimization of w values to measured catchment $\bar{E}$, followed by stepwise regression analysis	(Yang et al., 2007)
$n = 5.755\left(\frac{K_s}{\overline{i_r}}\right)^{-0.368} M^{0.292} e^{-5.428\tan\beta}$ and $n = 2.721\left(\frac{K_s}{\overline{i_r}}\right)^{-0.393} M^{-0.301} e^{4.351\tan\beta}$	K_s, saturated hydraulic conductivity $\overline{i_r}$, mean precipitation intensity in 24 hours M, vegetation coverage $\tan\beta$, average slope	Optimization of n values to measured catchment $\bar{E}$, followed by stepwise regression analysis	(Yang et al., 2009)
$n = 0.21\left(\frac{\kappa Z_r}{\alpha}\right) + 0.60$	κ, fractional plant-available water holding capacity Z_r, effective rooting depth α, mean depth per storm event	Optimization of n values to a soil moisture model at single aridity index value followed by linear regression	(Donohue et al., 2012)
$w = 2.36(M) + 1.16$	M, vegetation coverage	Optimization of w values to measured catchment $\bar{E}$, followed by linear regression	(Li et al., 2013)

Table S1: Continued.

Functional Forms	Parameters	Methodology	Reference
$w = F(PFC, PfE, Rr, ASD, CV_P)$	PFC, percentage of forest coverage PfE, number of months that peak precipitation follows peak potential evapotranspiration Rr, relief ratio ASD, average storm depth CV_P, coefficient of variation of precipitation	Optimization of w values to measured catchment $\bar{E}$, followed by multivariate adaptive regression splines (MARS)	(Shao et al., 2012)
$w = (-0.09322)lat + (0.13085)CTI + (1.31697)NDVI + (0.00003)A + (-0.00018)elev + 5.05722$ and $w = (-0.01042)lat + (0.146186)CTI + (2.81063)NDVI + 0.69387$ and $w = (-0.03288)lat + (-0.09311)slp + (1.12312)NDVI + (-0.00205)long + (-0.00026)elev + 3.50412$	lat, absolute latitude of basin center $long$, basin center longitude slp, slope gradient CTI, compound topographic index $NDVI$, normalized difference vegetation index A, drainage area $elev$, elevation	Optimization of w values to measured catchment $\bar{E}$, followed by stepwise multiple linear regression (MLR)	(Xu et al., 2013)

Table S1: Continued.

Functional Forms	Parameters	Methodology	Reference
$w = F(lat, slp, NDVI, long, elev)$	lat, absolute latitude of basin center $long$, basin center longitude slp, slope gradient $NDVI$, normalized difference vegetation index $elev$, elevation	Optimization of w values to measured catchment $\bar{E}$, followed by stepwise multiple linear regression (MLR) to select input variables to train a neural network	(Xu et al., 2013)
$n = 0.7078\left(\frac{\kappa Z_r}{\alpha}\right)^{0.5945}$	κ, fractional plant-available water holding capacity Z_r, effective rooting depth α, mean depth per storm event	Optimization of n values to a soil moisture model followed by curve fitting	(Cong et al., 2015)
$n = a\ln\left[\left(\frac{\kappa Z_r}{\alpha}\right)^2\right] + b\ln\left[\frac{\kappa Z_r}{\alpha}\right] + c$ where, $\begin{cases} a = -0.003\left(\log_{10}\frac{\overline{E_0}}{\overline{P}}\right)^2 + 0.247\log_{10}\frac{\overline{E_0}}{\overline{P}} + 0.19 \\ b = -0.022\frac{\overline{E_0}}{\overline{P}} + 0.403 \\ c = -0.071\left(\log_{10}\frac{\overline{E_0}}{\overline{P}}\right)^2 - 0.332\log_{10}\frac{\overline{E_0}}{\overline{P}} + 0.761 \end{cases}$	κ, fractional plant-available water holding capacity Z_r, effective rooting depth α, mean rainfall depth	Optimization of n values to a soil moisture model followed by curve fitting	(Yang et al., 2016; Zhang et al., 2018)
$w = 1 + (3.683)M^{0.798}e^{-(0.246)S}$	M, vegetation coverage S, climate seasonality index	Optimization of w values to measured catchment $\bar{E}$, followed by least squares regression.	(Ning et al., 2017)

Table S1: Continued.

Functional Forms	Parameters	Methodology	Reference
$w = F\left(\frac{AWC}{P}, rCMS, slope, SF\right)$	AWC, available soil water holding capacity $rCMS$, relative cumulative moisture surplus $slope$, mean watershed slope SF, fraction of annual precipitation falling as snow	Optimization of w values to measured catchment $\bar{E}$, followed by stepwise forward regression to build a generalized additive model	(Abatzoglou and Ficklin, 2017)
$n = (2.100)CI + (-0.157)SIM + (-0.284)PDSI + (-1.203)SI + (-45.4)Rr + 1.299$	CI, precipitation concentration index SIM, Milly's index of seasonality $PDSI$, Palmer drought severity index SI, seasonality index of precipitation Rr, relief ratio	Optimization of n values to measured catchment $\bar{E}$, followed by multiple stepwise regression (MSR)	(Xing et al., 2018)
$n = F(M, ASD, Cv, SI, PDSI, IA, CA)$	M, vegetation coverage ASD, average storm depth Cv, coefficient of variation of precipitation SI, seasonality index of precipitation $PDSI$, Palmer drought severity index IA, effective irrigated area ratio CA, cultivated land area ratio	Optimization of n values to measured catchment $\bar{E}$, followed by multivariate adaptive regression splines (MARS)	(Xing et al., 2018)

Table S1: Continued.

Functional Forms	Parameters	Methodology	Reference
$\omega = 1.8077 + (0.1856)CTI - (1.4551)NDVI + (0.4489)RFL + (0.5542)SI$	CTI, compound topographic index $NDVI$, normalized difference vegetation index RFL, the ratio of farmland area to total basin area SI, seasonality index of precipitation	Optimization of w values to measured catchment $\bar{E}$, followed by multiple linear regression	(Bai et al., 2019)
$w = F(CTI, NDVI, RFL, SI)$	CTI, compound topographic index $NDVI$, normalized difference vegetation index RFL, the ratio of farmland area to total basin area SI, seasonality index of precipitation	Optimization of w values to measured catchment $\bar{E}$, followed by calibration of an artificial neural network	(Bai et al., 2019)
$w = 1 + (3.67)M^{0.27}e^{-(0.21)SAI}$	M, vegetation coverage SAI, climate seasonality and asynchrony index	Optimization of w values to measured catchment $\bar{E}$, followed by a stepwise regression method.	(Ning et al., 2019)
$w = 1 + (25.03)M^{0.43}f_s^{0.71}$	M, vegetation coverage f_s, fraction of precipitation falling as snow	Optimization of w values to measured catchment $\bar{E}$, followed by a stepwise regression method and parameter reduction due to collinearity.	(Ning et al., 2019)

5

Table S1: Continued.

Functional Forms	Parameters	Methodology	Reference
w **or** $n = F\left(X_1(t), X_2(t), X_3(t)\right)$	$X_1(t)$, time varying per capita gross regional product $X_2(t)$, time varying mean annual temperature $X_3(t)$, time varying mean annual precipitation	Optimization of w/n values to measured catchment $\bar{E}$, followed by a hierarchical Bayesian calibration of constant and time varying regression models for the catchment-specific parameter	(Zhang et al., 2019)
$w = -(2.23)\ln[S_t] - (4.34)\ln[NDVI_t] - (9.77)\ln[T_{maxt}] + (0.82)\ln[P_t] - 27.55$	S_t, 11-year average of annual sunshine duration $NDVI_t$, 11-year average of annual normalized difference vegetation index T_{maxt}, 11-year average of annual maximum temperature P_t, 11-year average of annual precipitation	Optimization of w values to measured catchment $\bar{E}$, followed by a stepwise regression method.	(Li et al., 2020b)
$w = -2.328 - (8.220)URBN + (7.429)\ln[IA] + (1.211)e^{CA} + (5.324)e^{T} - (2.069)e^{PET}$	$URBN$ constructed land area rate IA, irrigated area rate CA, cultivated area rate T, temperature PET, potential evapotranspiration	Optimization of w values to measured catchment $\bar{E}$, followed by a stepwise regression method. This catchment-specific parameter for the "Budyko-like" equation of (Zhang et al., 2001)	(Li et al., 2020a)
$\Delta w = (0.63)\Delta F - 0.03$	ΔF, change in forest cover	Optimization of Δw values to measured catchment $\overline{\Delta E}$, followed by linear regression.	(Ning et al., 2020a)

Table S1: Continued.

Functional Forms	Parameters	Methodology	Reference
$w = 1 + (4.49)M^{0.73}e^{-(0.33)SAI}$	M, vegetation coverage SAI, climate seasonality and asynchrony index	Modification of an expression from (Ning et al., 2017).	(Ning et al., 2020b)
$w = F\left(\frac{E}{P}, \frac{E_p}{P}, SI, BF, SM, NDVI, AO, PDO, Niño\ 3.4, Sunspots, EIA\right)$	$\frac{E}{P}$, evaporative index $\frac{E_p}{P}$, aridity index SI, seasonality index of precipitation SM, Soil moisture of the basin BF, baseflow of the basin $NDVI$, normalized difference vegetation index AO, Arctic Oscillation PDO, Pacific Decadal Oscillation $Niño\ 3.4$, The area averaged SST from 5ºS to 5ºN and 170º–120ºW calculated from the HadISST1 data $Sunspots$, Solar activity EIA, Effective irrigated area in the study area	Optimization of w values to measured catchment $\bar{E}$, followed by a correlation analysis and partial correlation analysis.	(Zhao et al., 2020)